BIOCHEMISTRY
including biophysical chemistry & molecular biology

Rapid Report

pubs.acs.org/biochemistry

Crystal Structure of the Redox-Active Cofactor Dibromothymoquinone Bound to Circadian Clock Protein KaiA and Structural Basis for Dibromothymoquinone's Ability to Prevent Stimulation of KaiC Phosphorylation by KaiA

Rekha Pattanayek, Said K. Sidiqi, and Martin Egli*

Department of Biochemistry, Vanderbilt University, School of Medicine, Nashville, Tennessee 37232, United States

Supporting Information

ABSTRACT: KaiA protein that stimulates KaiC phosphorylation in the cyanobacterial circadian clock was recently shown to be destabilized by dibromothymoquinone (DBMIB), thus revealing KaiA as a sensor of the plastoquinone (PQ) redox state and suggesting an indirect control of the clock by light through PQ redox changes. Here we show using X-ray crystallography that several DBMIBs are bound to KaiA dimer. Some binding modes are consistent with oligomerization of N-terminal KaiA pseudoreceiver domains and/or reduced interdomain flexibility. DBMIB bound to the C-terminal KaiA (C-KaiA) domain and limited stimulation of KaiC kinase activity by C-KaiA in the presence of DBMIB demonstrate that the cofactor may weakly inhibit KaiA-KaiC binding.

In the photosynthetic cyanobacterium *Synechococcus elongatus* (*S. elongatus*) the KaiA, KaiB, and KaiC proteins constitute a post-translational circadian oscillator (PTO).[1−4] The discovery that regular patterns of KaiC phosphorylation and dephosphorylation with a period of 24 h are generated when the three proteins are incubated in a test tube in the presence of ATP,[5] rendered this system an attractive target for biochemical and biophysical investigations of the inner workings of a molecular clock. The central cog, KaiC, exhibits autophosphorylation and -dephosphorylation[6,7] as well as ATPase activities.[8] Dephosphorylation proceeds via a phosphotransferase mechanism that returns phosphates from Ser and Thr back to ADP, thus endowing KaiC with an ATP synthase activity.[9] KaiA enhances KaiC phosphorylation,[10,11] and KaiB antagonizes KaiA action.[11,12]

The input and output pathways of the clock comprise a variety of factors that transmit environmental cues to the inner timer and deliver temporal information based on the phosphorylation loop to downstream cellular processes that include clock-controlled gene expression, respectively (reviewed in refs 3 and 4). Proteins participating in the input pathway that have been characterized to date include LdpA[13,14] and CikA.[15,16] Both are redox-active factors; CikA is a histidine kinase and LdpA is an iron sulfur protein. CikA was shown to be required for resetting of the phase after a dark pulse,[15] and mutations in the protein resulted in shortened periods of the oscillator and altered patterns of KaiC phosphorylation.

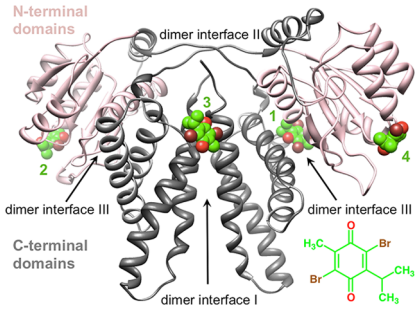

Figure 1. Overall view of the crystal structure of the *S. elongatus* KaiA:DBMIB complex. The KaiA dimer is depicted in a secondary structure cartoon mode, and the oxidized form of DBMIB is shown at the bottom right, with carbon, oxygen, and bromine atoms colored in light green, red, and brown, respectively. N- (residues 1−139) and C-terminal (residues 140−282) domains of KaiA are colored in pink and gray, respectively, and are labeled along with dimer interfaces. Bound DBMIBs are shown in space filling mode and are numbered 1−4.

The brominated and water-soluble plastoquinone (PQ) analogue 2,5-dibromo-3-methyl-6-isopropyl-*p*-benzoquinone (DBMIB; Figure 1)[17] was found to destabilize both LdpA and CikA.[14] The so-called pseudoreceiver (PsR) domain of CikA is able to bind DBMIB and a series of additional quinone analogues,[18,19] thus implicating this His kinase in indirect information transfer on the light environment to the central cyanobacterial timer via redox changes in bound quinone.[18]

A more recent study also established binding between the PsR domain of KaiA and DBMIB and therefore provided evidence for KaiA acting as a sensor of environmental signals and modulating the circadian clock as a result of changes in the redox state.[20] Accordingly, the oxidized but not the reduced form of DBMIB binds to KaiA and induces protein oligomerization, ultimately preventing KaiA from binding to KaiC and stimulating phosphorylation of the latter.[20] KaiA forms a domain-swapped dimer[21] (Figure 1), whereby the N-terminal domains (N-KaiA) adopt a PsR-like fold[11,21] and the C-terminal α-helical bundle domains (C-KaiA)[22,23] are responsible for dimerization and KaiC binding.[24] Native polyacrylamide gel electrophoresis (PAGE) in conjunction

Received: July 25, 2012
Revised: September 26, 2012
Published: September 28, 2012

   dx.doi.org/10.1021/bi301222t | *Biochemistry* 2012, 51, 8050−8052

with NMR solution experiments supported binding of DBMIB to the N-KaiA PsR domain as the underlying cause of protein aggregation.[20] Conversely, lack of mobility changes in native PAGE assays of mixtures of C-KaiA and DBMIB appeared to argue against an involvement of this domain in light-induced control of the clock mediated by KaiA. However, this study did not characterize the binding modes of DBMIB in detail.

To establish the precise KaiA binding sites and coordination modes of DBMIB, we determined the crystal structure of full-length *S. elongatus* KaiA soaked in a solution of the oxidized form of DBMIB at a resolution of 2.38 Å (see the Supporting Information for experimental details, Table S1 for refinement parameters, Figures S1 and S2 for the quality of the final electron density, Figure S3 for KaiA loop conformations, and Figure S4 for a temperature factor analysis). We established four unique binding sites for DBMIB (DBMIBs 1−4; Figure 1), such that each KaiA dimer in the crystal is surrounded by eight DBMIB molecules (Figure S5 in the Supporting Information; the KaiA dimer does not adopt crystallographic 2-fold symmetry). DBMIB 1 is located between the N- and C-KaiA domains from different subunits at dimer interface III. DBMIBs 2 and 4 are interacting mainly with N-KaiA, but like molecule 1, they establish contacts to domains from symmetry-related KaiAs. By contrast, DBMIB 3 is bound at dimer interface I of C-KaiA domains and is exclusively associated with one KaiA dimer (Figure 1), thus revealing an unexpected binding mode.

Closer examination of the binding modes of DBMIB molecules reveals common features and a preference for a particular folding topology (Figure S6 in the Supporting Information). In all four cases, the quinone analogue sits adjacent to the N-terminus of an α-helix that is preceded by a turn involving proline (Figures 1 and 2). For DBMIBs 1, 2, and 4, the turn is between a β-strand and the α-helix and DBMIB 3 sits close to a turn between α-helices. Whereas P115a is located at some distance from DBMIB 1 (Figure 2A), DBMIB 3 actually stacks onto P229a (Figure 2C) and DBMIBs 2 and 4 are associated with P61b and P61a, respectively (Figure 2B,D). With DBMIB 1 and DMBIB 4, a lysine and an arginine, respectively, snake along the aromatic moiety of the binder, thus providing a hydrophobic platform. In two cases there is potential for formation of a halogen bond involving close vicinity (<3.3 Å) between an electronegative moiety (keto or caboxylate oxygen) and bromine (asterisk in Figure 2 A,B). Further, DBMIBs 2 and 4 are adjacent to newly built loops in the complex structure [missing in the native KaiA structure[21] (Figure S3 in the Supporting Information)] and establish

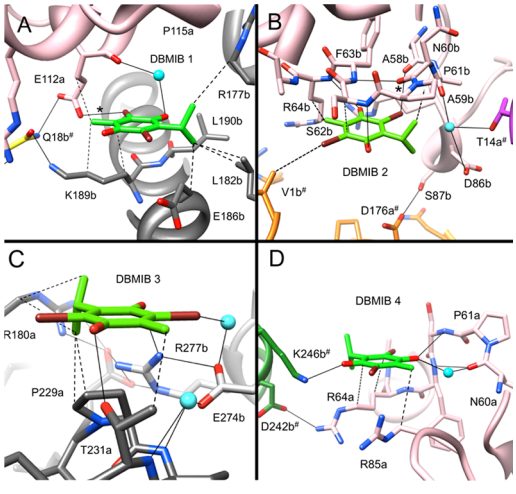

Figure 2. Coordination modes of DBMIB molecules (A) 1, (B) 2, (C) 3, and (D) 4 to KaiA. The coloring of N-KaiA and C-KaiA domains in the original dimer matches that in Figure 1. Residues belonging to four different symmetry-related KaiA dimers are highlighted in yellow (A), orange and magenta (B), and green (D). Selected side chains are depicted with oxygen in red and nitrogen in blue and are labeled (a and b indicate subunits and # indicates a symmetry mate). Hydrogen bonds are indicated by thin solid lines, putative halogen bonds are marked with an asterisk, and hydrophobic contacts as well as a van der Waals contact by bromine (panel B) are indicated by dashed lines.

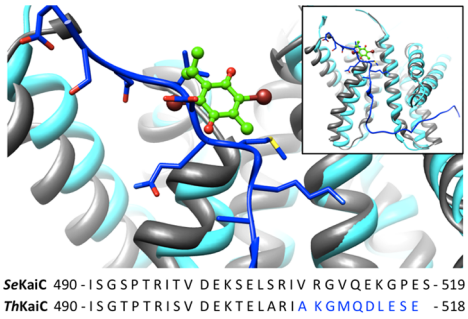

Figure 3. Putative clash between DBMIB 3 coordinated between C-terminal domains of the KaiA dimer (see panel C of Figure 2 for a close-up) and a portion of a KaiC C-terminal peptide bound to KaiA dimer (see inset for an overall view). The NMR structure of the *Thermosynechococcus elongatus* (*T. elongatus*) C-KaiA dimer (cyan) bound to the last 30 residues of KaiC (blue)[24] was superimposed onto the C-KaiA portion with DBMIB 3 bound as observed in our crystal structure (gray). Sequences of the C-terminal stretches of KaiCs from *S. elongatus* and *T. elongatus* are shown at the bottom. In the crystal structure of *S. elongatus* KaiC hexamer,[25] one of the C-terminal tails exhibits a conformation very similar to that seen for the peptide in the solution structure of the *T. elongatus* KaiA:KaiC peptide complex. DBMIB coordinated at that site would interfere with binding of the last 10 residues of KaiC (highlighted in blue in the sequence) and result in overlaps with the backbone and side chains from at least five amino acids. As in the case of *S. elongatus* KaiA, DBMIB causes aggregation of *T. elongatus* KaiA. However, addition of DBMIB to the KaiB protein from either organism has no effect at all (Figures S7 and S8 in the Supporting Information).

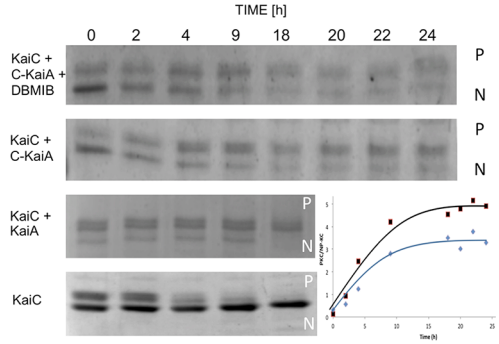

Figure 4. SDS-PAGE assay of *S. elongatus* KaiC phosphorylation, separating the more slowly migrating phosphorylated form (P) from the nonphosphorylated form (N). From top to bottom: KaiC, C-KaiA and oxidized form of DBMIB; KaiC and C-KaiA; KaiC and full-length KaiA (KaiA stimulates KaiC phosphorylation more strongly than C-KaiA); and KaiC alone (KaiC autodephosphorylates without KaiA). DBMIB affects C-KaiA action as indicated by the lower P-KaiC/KaiC ratio (blue) compared to that ratio in the absence of DBMIB (black; graph at bottom right).

dx.doi.org/10.1021/bi301222t | *Biochemistry* 2012, 51, 8050−8052

indirect or direct contacts with a residue from the loop (i.e., S87b, DBMIB 2, and R85a, DMBIB 4, respectively).

In addition to the above similarities, there are a number of differences between the binding modes of individual DBMIB molecules. For example, DBMIB 1 is wedged between two antiparallel amide moieties, the top one contributed by E112a and the bottom one by K189b, such that the keto oxygen of E112a establishes a water-mediated contact to a DBMIB keto oxygen (Figure 2A). In the case of DBMIB 2, a tight turn in the N-KaiA backbone sits atop the aromatic moiety and amide N−H groups from S62b and R64b (Figure 2B) are directed toward DBMIB keto oxygens. An N−H from a third residue (F63b) forms a hydrogen bond to the keto oxygen from N60b three residues away, thus tying together the turn, with the hydrogen bond positioned more or less parallel to the DBMIB ring.

The locations of DBMIB binding sites allow a more detailed understanding of the cofactor's mode of action in terms of transmitting environmental cues, i.e., light conditions, to the KaiABC timer. Residues from the N-KaiA PsR-like domain are responsible for the majority of interactions seen for DBMIBs 1, 2, and 4 (Figure 2; N-KaiA domains of the original dimer in the crystal are colored in pink). Residues interacting with DBMIB (i.e., E112a and K189b; DBMIB 1), closely associated with DBMIB (i.e., A59b, water-mediated; DBMIB 2) or DBMIB atoms themselves (i.e., Br2, DBMIB 2) then establish contacts to N-KaiA domains from symmetry mates, consistent with the aggregation model.[20] The coordination site observed for DBMIB 1, stitching together PsR N-KaiA and C-KaiA domains (Figure 2A), and the improved ordering of loops directly associated with cofactor binding (DBMIB 2, 4; Figure 2B,D) are also consistent with reduced flexibility and aggregation.

The association of DBMIB 3 exclusively with C-KaiA domains prompted us to examine an additional mode of interference of DBMIB with KaiA-stimulated phosphorylation of KaiC. The binding site of DBMIB 3 overlaps with a portion of the binding interface between KaiC C-terminal peptide and KaiA dimer[24] (Figure 3) but cannot be expected to result in a bandshift in native PAGE.[20] Whereas the structure of the C-KaiA:KaiC peptide complex in solution discloses binding of two peptides per KaiA dimer,[24] in the crystal the site equivalent to the one occupied by DBMIB 3 on the opposite side of the dimer is sealed off by a lattice contact between KaiA symmetry mates. SDS-PAGE assays of C-KaiA-stimulated KaiC phosphorylation in the presence and absence of the oxidized form of DBMIB reveal a slightly impaired activity of KaiA in the former case (Figure 4, top two panels), providing support for DBMIB affecting KaiC-peptide binding.

In summary, the binding modes of three of the DBMIBs visualized in the structure of the KaiA:DBMIB complex are consistent with N-KaiA PsR-domain aggregation[20] and reduced KaiA interdomain flexibility. The newly discovered DBMIB associated with C-KaiA alone together with the reduced ability of this domain to enhance KaiC phosphorylation in the presence of DBMIB suggest a more complex involvement of the cofactor in the mediation of the clock's light input pathway.

■ ASSOCIATED CONTENT

Supporting Information

Methods and materials, Table S1, and Figures S1−S8. This material is available free of charge via the Internet at http://pubs.acs.org.

Accession Codes

The PDB code (http://www.rcsb.org) for the complex is 4G86.

■ AUTHOR INFORMATION

Corresponding Author

*Phone: (615) 343-8070. Fax: (615) 322-7122. E-mail: martin.egli@vanderbilt.edu.

Funding

Supported by NIH Grant R01 GM073845. Use of the APS was supported by the U.S. Dept. of Energy, Office of Science, Office of Basic Energy Sciences, Contract No. DE-AC02-06CH11357.

Notes

The authors declare no competing financial interest.

■ REFERENCES

(1) Ishiura, M., Kutsuna, S., Aoki, S., Iwasaki, H., Andersson, C. R., Tanabe, A., Golden, S. S., Johnson, C. H., and Kondo, T. (1998) *Science 281*, 1519−1523.

(2) Johnson, C. H., Egli, M., and Stewart, P. L. (2008) *Science 322*, 697−701.

(3) Ditty, J. L., Mackey, S. R., Johnson, C. H., Eds. (2009) *Bacterial Circadian Programs*, Springer Publishers Inc., Heidelberg, Germany.

(4) Johnson, C. H., Stewart, P. L., and Egli, M. (2011) *Annu. Rev. Biophys. 40*, 143−167.

(5) Nakajima, M., Imai, K., Ito, H., Nishiwaki, T., Murayama, Y., Iwasaki, H., Oyama, T., and Kondo, T. (2005) *Science 308*, 414−415.

(6) Nishiwaki, T., Iwasaki, H., Ishiura, M., and Kondo, T. (2000) *Proc. Natl. Acad. Sci. U.S.A. 97*, 495−499.

(7) Xu, Y., Mori, T., and Johnson, C. H. (2003) *EMBO J. 22*, 2117−2126.

(8) Terauchi, K., Kitayama, Y., Nishiwaki, T., Miwa, K., Murayama, Y., Oyama, T., and Kondo, T. (2007) *Proc. Natl. Acad. Sci. U.S.A. 104*, 16377−16381.

(9) Egli, M., Mori, T., Pattanayek, R., Xu, Y., Qin, X., and Johnson, C. H. (2012) *Biochemistry 51*, 1547−1558.

(10) Iwasaki, H., Nishiwaki, T., Kitayama, Y., Nakajima, M., and Kondo, T. (2002) *Proc. Natl. Acad. Sci. U.S.A. 99*, 15788−15793.

(11) Williams, S. B., Vakonakis, I., Golden, S. S., and LiWang, A. C. (2002) *Proc. Natl. Acad. Sci. U.S.A. 99*, 15357−15362.

(12) Kitayama, Y., Iwasaki, H., Nishiwaki, T., and Kondo, T. (2003) *EMBO J. 22*, 1−8.

(13) Katayama, M., Kondo, T., Xiong, J., and Golden, S. S. (2003) *J. Bacteriol. 185*, 1415−1422.

(14) Ivleva, N. B., Bramlett, M. R., Lindahl, P. A., and Golden, S. S. (2005) *EMBO J. 24*, 1202−1210.

(15) Schmitz, O., Katayama, M., Williams, S. B., Kondo, T., and Golden, S. S. (2000) *Science 289*, 765−768.

(16) Zhang, X., Dong, G., and Golden, S. S. (2006) *Mol. Microbiol. 60*, 658−668.

(17) Trebst, A. (1980) *Methods Enzymol. 69*, 675−715.

(18) Ivleva, N. B., Gao, T., LiWang, A. C., and Golden, S. S. (2006) *Proc. Natl. Acad. Sci. U.S.A. 103*, 17468−17473.

(19) Gao, T., Zhang, X., Ivleva, N. B., Golden, S. S., and LiWang, A. (2007) *Protein Sci. 16*, 465−475.

(20) Wood, T. L., Bridwell-Rabb, J., Kim, Y.-I., Gao, T., Chang, Y.-G., LiWang, A., Barondeau, D. P., and Golden, S. S. (2010) *Proc. Natl. Acad. Si. U.S.A. 107*, 5804−5809.

(21) Ye, S., Vakonakis, I., Ioerger, T. R., LiWang, A. C., and Sacchettini, J. C. (2004) *J. Biol. Chem. 279*, 20511−20518.

(22) Garces, R. G., Wu, N., Gillon, W., and Pai, E. F. (2004) *EMBO J. 23*, 1688−1698.

(23) Vakonakis, I., Sun, J., Wu, T., Holzenburg, A., Golden, S. S., and LiWang, A. C. (2004) *Proc. Natl. Acad. Sci. U.S.A. 101*, 1479−1484.

(24) Vakonakis, I., and LiWang, A. C. (2004) *Proc. Natl. Acad. Sci. U.S.A. 101*, 10925−10930.

(25) Pattanayek, R., Williams, D. R., Pattanayek, S., Xu, Y., Mori, T., Johnson, C. H., Stewart, P. L., and Egli, M. (2006) *EMBO J. 25*, 2017−2038.

Supporting Information

Crystal structure of the redox-active cofactor DBMIB bound to circadian clock protein KaiA and structural basis for DBMIB's ability to prevent stimulation of KaiC Phosphorylation by KaiA

Rekha Pattanayek, Said K. Sidiqi, and Martin Egli*

Department of Biochemistry, Vanderbilt University, School of Medicine, Nashville, TN 37232
*Contact: Tel: (615) 343-8070; Fax: (615) 322-7122; E-mail: martin.egli@vanderbilt.edu

Table of Contents:

Protein expression and purification

The *S. elongatus* KaiA, KaiB and KaiC GST fusion proteins were overexpressed in *Escherichia coli* (BL21 cell line, Novagen) and purified following previously described protocols.[1] The C-KaiA protein (amino acids 180 to 284) was subcloned from KaiA into a pET-*Se*KaiA-C$(His)_6$ vector and overexpressed in *E. coli* (Rosetta2[DE3]). The protein was purified following previously described protocols.[2] The *T. elongatus* KaiA and KaiB proteins were expressed and purified as described in refs. 3 and 4, respectively. The quality of all proteins was assessed by SDS-PAGE (4-20%, BioRad).

Crystallization and crystal soaking experiments

The KaiA protein buffer (50 mM Tris pH 7.8 and 150 mM NaCl) was exchanged with 20 mM Hepes pH 7.5 and 20 mM NaCl for crystallization. The protein concentration was ca. 12 mg/mL. KaiA crystals were grown using the hanging drop vapor diffusion technique following published conditions.[5] The reservoir solution was 140 to 180 mM ammonium sulfate, 85 mM sodium cacodylate pH 6.8, 20% PEG 8000 and 15% glycerol. Equal volumes of the protein and reservoir solutions were mixed and the droplets equilibrated against 0.75 mL of reservoir solution. Crystals grew within a few days at a temperature of 20°C and were subsequently soaked in the cryo solution (reservoir solution with 25% glycerol added) containing various amounts of DBMIB (1 to 10 mM) and using different soaking times (1 to 16 hours). Soaked KaiA crystals were mounted in cryo loops and stored in liquid nitrogen prior to data collection. X-ray data were collected for crystals soaked under various conditions and the data used for the structural analysis were obtained from a crystal soaked in a 1 mM DBMIB solution for two hours. The crystals used for structural analysis showed no obvious defects (i.e. cracks) under a light microscope and resolution and quality of the diffraction data were superior to data from crystals that were soaked for longer periods of time.

X-ray data collection, structure determination and refinement

X-ray diffraction data were collected on the 21-ID-G beam line of the Life Sciences Collaborative Access Team (LS-CAT) at the Advanced Photon Source (APS), located at Argonne National Laboratory (Argonne, IL), using a MARCCD 300 detector at a wavelength of 0.98 Å. The crystals were kept at 110 K during data collection. Diffraction data were integrated,

scaled and merged with HKL2000.[6] Selected data collection and refinement statistics are listed in **Table S1**. The structure was determined by Molecular Replacement with the program CNS[7] using the crystal structure of the KaiA dimer from *S. elongatus* (PDB ID 1R8J) as the search model.[5] CNS was used for initial rigid body refinement and all subsequent refinement was performed with PHENIX,[8] setting aside 5% of reflections to calculate the R-free. Manual rebuilding of the model was done in Coot.[9] Four DBMIB molecules were identified in Fourier $2F_o$-F_c difference electron density maps. B-factors and DBMIB occupancies were refined in separate cycles of optimization. Examples of the quality of the final electron density are depicted in **Figure S1** (DBMIBs) and **Figure S2** (selected loop regions) and refinement statistics are summarized in **Table S1**. Loop regions that were absent in the native structure were completely built (**Figure S3**) and in addition to 179 water molecules, two glycerol molecules and two partial PEG molecules were also identified in electron density maps and incorporated into the final model. A model of the KaiA dimer in cartoon mode with main chain atoms colored according to the regional B-factors is depicted in **Figure S4**.

KaiC phosphorylation assays

KaiC phosphorylation assays using either full-length KaiA and or the C-terminal domain (C-KaiA) in the presence or absence of DBMIB as shown in **Figure 4** were performed following the published work by Wood and coworkers.[10]

A) *S. elongatus* C-KaiA, *S. elongatus* KaiC and oxidized DBMIB: A solution of 150 µL of purified C-KaiA (0.18 µg/µL) containing 280 µM of DBMIB (Sigma-Aldrich) was mixed with 360 µL reaction buffer (20 mM Tris-HCl pH 8, 150 mM NaCl, 0.5 mM EDTA, 5 mM $MgCl_2$ and 5mM ATP). Following incubation of the sample at room temperature for 15 minutes, 300 µL of a KaiC solution (0.6 µg/µL) were added. The sample was then incubated at 30°C for 24 hours, whereby 60 µL aliquots were collected at various intervals (0, 2, 4, 9, 12, 18, 22 and 24 hours).

B) *S. elongatus* C-KaiA and KaiC: The phosphorylation experiment described in A but without DBMIB was performed as a control experiment.

C) Full-length *S. elongatus* KaiA and KaiC. The phosphorylation assay was performed by adding a solution of 112 µL of purified KaiA (0.41 µg/µL) to 35 µL reaction buffer.

Following incubation at room temperature for 15 minutes, 360 µL of KaiC solution (0.47 µg/µL) were added and the sample incubated and aliquots collected as described in A.

D) *S. elongatus* KaiC auto-phosphorylation was assayed in the absence of KaiA and DBMIB.

All samples were analyzed by 8% large SDS-PAGE. Gels were stained in a solution produced from one Phastgel Blue R tablet dissolved in 10% acetic acid and 50% methanol. A solution of 20% methanol and 10% acetic acid was used to destain the gel. Gel images were taken using a Bio Rad Gel Doc EZ imager with Image Lab 3.0 software. Intensities of individual bands were quantified with the program ImageJ (US NIH).[11]

KaiA and KaiB aggregation assays

Native PAGE experiments. Gels (4-25 %) with KaiA and KaiB proteins from *S. elongatus* and *T. elongatus* incubated in a 1mM DBMIB solution for 16 hours along with the controls (no DBMIB) were run using the Phast System and stained with Coomassie blue (GE Health Care).

Dynamic light scattering (DLS). The KaiA and KaiB proteins from *S. elongatus* (*Se*) were incubated in a 1mM DBMIB solution for 2 hours and compared to controls lacking DBMIB. All scattering experiments were performed at room temperature using a DynaPro 99 instrument (Protein Solutions Inc.). The buffer was 50 mM Tris•HCl pH 7.5 and 150 mM NaCl and protein concentrations varied between 1.5 and 2.5 mg/mL. The scattering values are the averages of 30 scans, each including 20 different time points. Data were analyzed with Dynamics software (version 5.5; Protein Solutions Inc.). Selected DLS statistics are summarized below and illustrated in **Figure S8**.

Protein	$\mathbf{D_T}^a$ [10^{-9} cm^2/s]	$\mathbf{R_H}^b$ [nm]	**Mass** [kDa]
*Se*KaiA	708.3	3.504	63.3
*Se*KaiA, DBMIB	38.0 (avg.)	54.9 (avg.)	4.0 x 10^4 (avg.)
*Se*KaiB	684.6	3.541	64.9
*Se*KaiB, DBMIB	698.9	3.511	63.6

a D_T, translational diffusion coefficient
b R_H, hydrodynamic radius

Data deposition

Atomic coordinates and structure factor data for the KaiA:DBMIB complex have been deposited in the Protein Data Bank (http://www.rcsb.org, entry code 4G86).

Table S1. Selected crystal data, data collection and refinement parameters.

Crystal data	
Space group	$P2_1$
No. KaiA molecules per asymmetric unit	2
a, *b*, *c* [Å]; β [°]	47.25, 126.35, 56.38; 114.4
Data collection	
No. of unique reflections	23,630
Resolution [Å] (last shell)	2.38 (2.42 – 2.38)
Completeness [%] (last shell)	97.9 (68.5)
R-merge [%] (last shell)	13.4 (46.4)
Refinement	
R-work (last shell)	0.218 (0.227)
R-free (last shell)	0.265 (0.304)
No. of non-hydrogen atoms	4,813
No. of DBMIB molecules	4
No. of water molecules	178
No. of glycerol / partial PEG molecules	2 / 2
Temperature factors:	average, minimum, maximum
All atoms [$Å^2$]	41.3, 17.5, 88.2
DBMIB [$Å^2$]	46.9, 24.4, 69.5
Occupancy DBMIBs 1-4	0.7
R.m.s. deviations:	
Bond lengths [Å]	0.005
Bond angles [°]	1.0
Ramachandran regions:	
Favored [%]	93.5
Allowed [%]	4.1
Generously allowed [%]	2.4

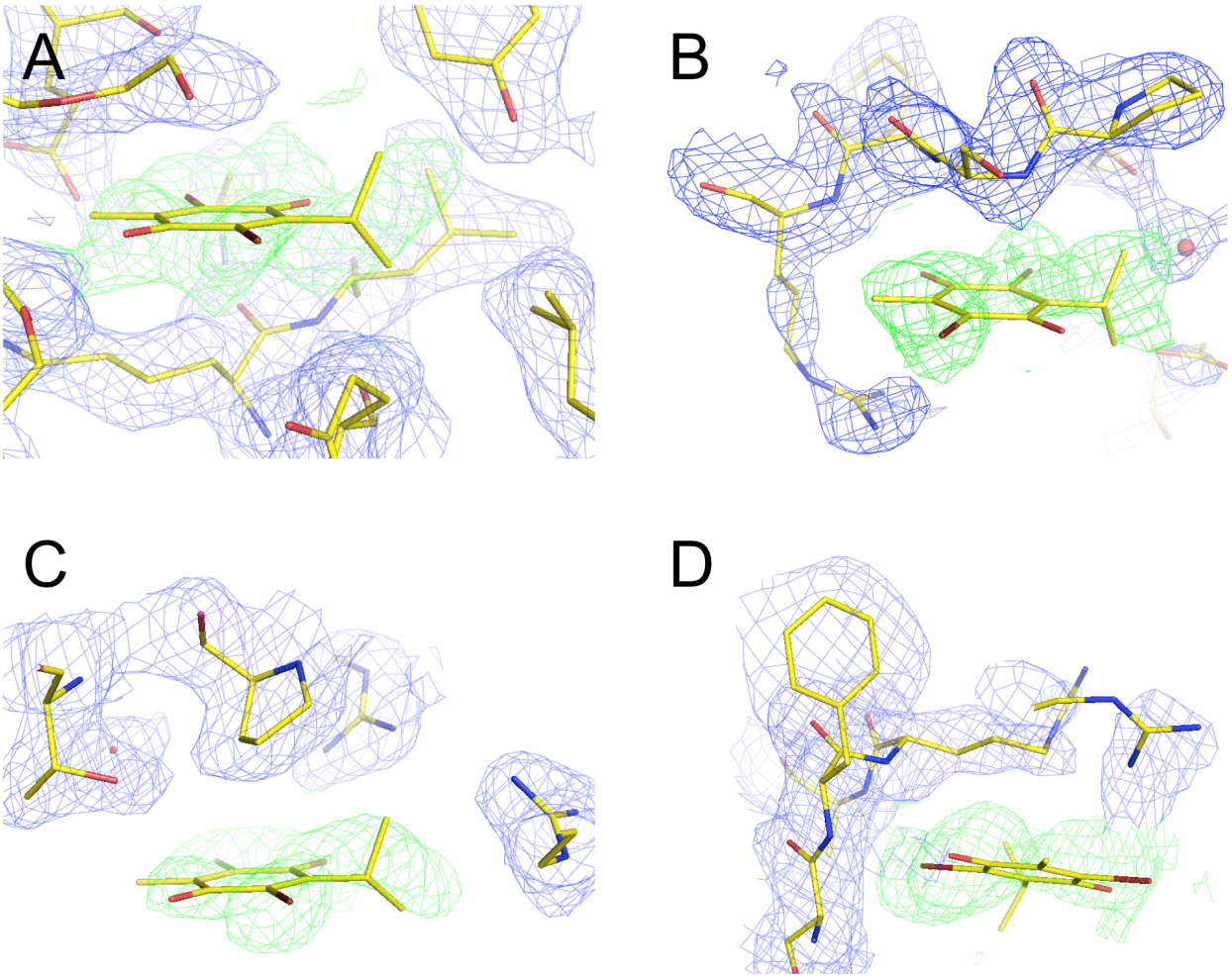

Figure S1. Quality of the final Fourier $2F_o$-F_c sum (blue) and omit (green; calculated in the absence of DBMIB) electron densities in the region of (A) DBMIB 1, (B) DBMIB 2, (C) DBMIB 3, and (D) DBMIB 4. The maps are drawn at the 1.0 σ level and water molecules are shown as red spheres. The figure was generated with the program Pymol.[12]

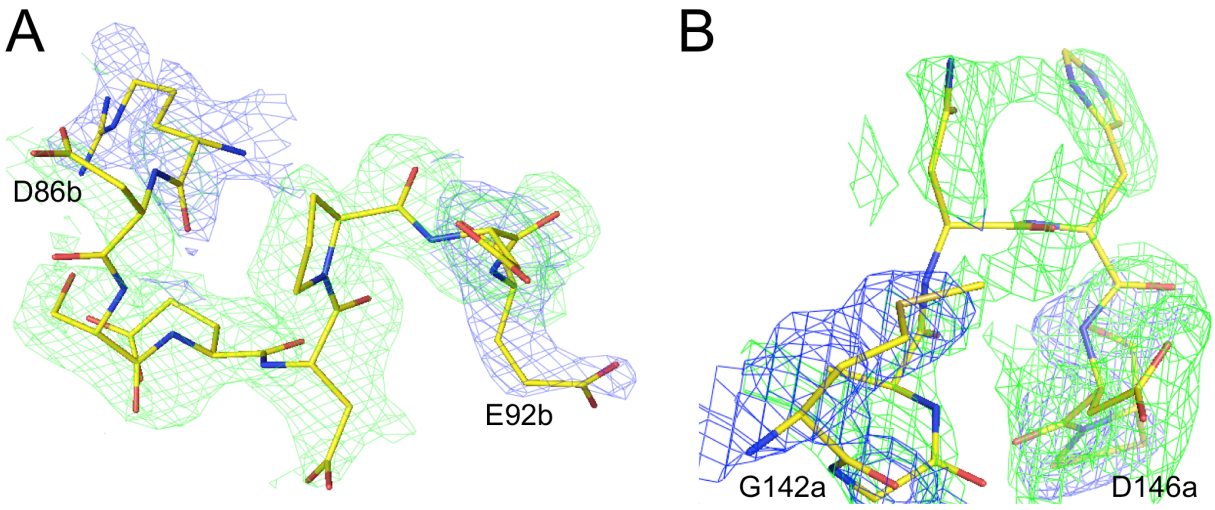

Figure S2. Quality of the final Fourier $2F_o$-F_c sum (blue) and omit (green) electron densities for loop regions comprising residues (A) D86 to E92 (B chain) and (B) G142 to D146 (A chain). The maps are drawn at the 1.0 σ level. The figure was generated with the program Pymol.[12]

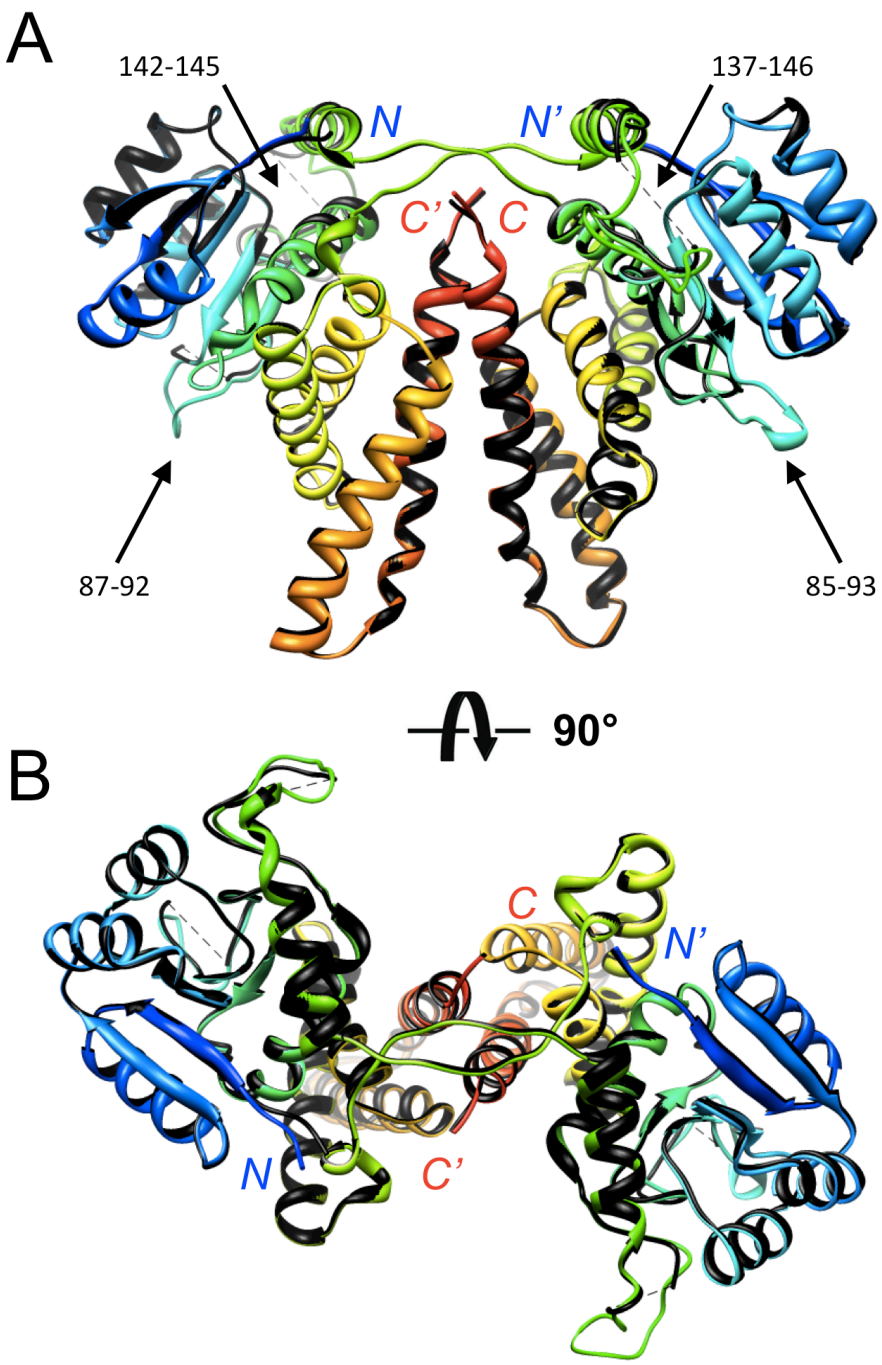

Figure S3. Superimposition of the crystal structures of domain-swapped *S. elongatus* KaiA dimer[8] (black ribbon) and KaiA:DBMIB complex (this work; rainbow coloring), viewed (A) roughly perpendicular to the C-terminal α-helical bundles and (B) rotated around the horizontal by 90°. Portions of loops missing in the original structure and completely built in the structure of the complex are indicated with dashed lines and arrows with residues numbered, respectively. The drawing was generated with the program UCSF Chimera.[13]

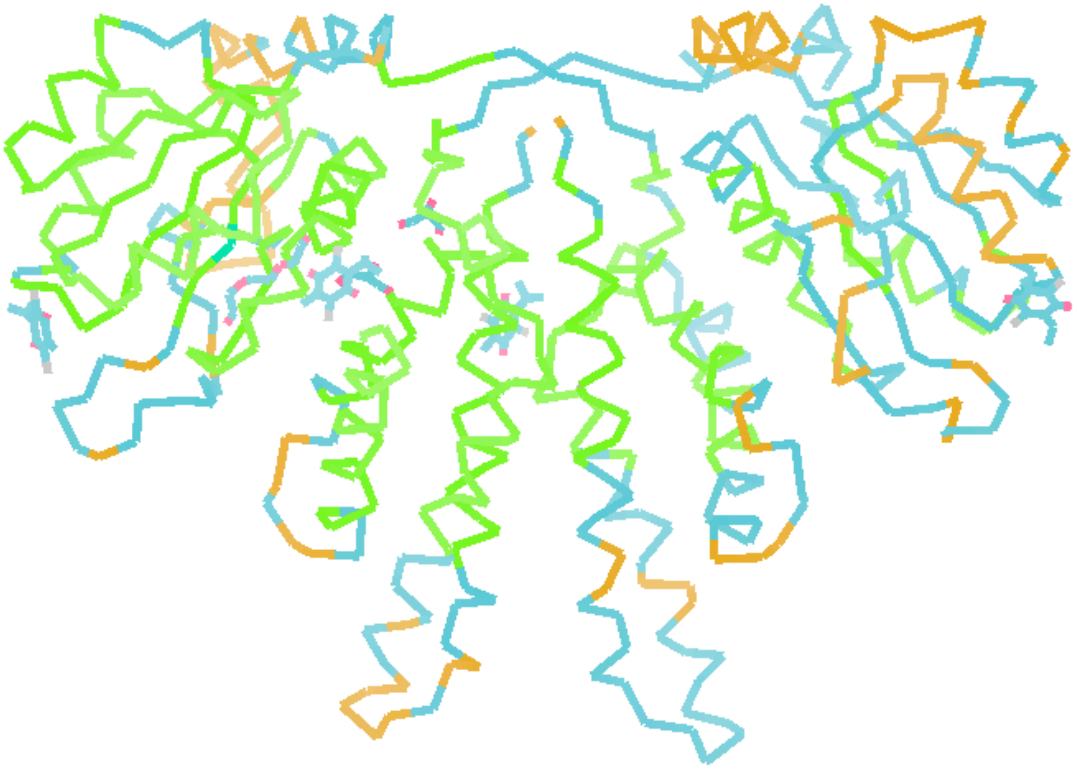

Figure S4. The crystal structure of *S. elongatus* KaiA dimer:DBMIB complex with the Cα-atom chain and carbon atoms of DBMIB, glycerol and PEG molecules colored according to atomic B-factor values (green < blue < yellow). Oxygen atoms of DBMIB, glycerol and PEG are red and DBMIB bromines are gray. The dimer is rotated by ca. 180° around the vertical relative to the orientation in **Figure 1**. The figure was generated with the program Coot.[9]

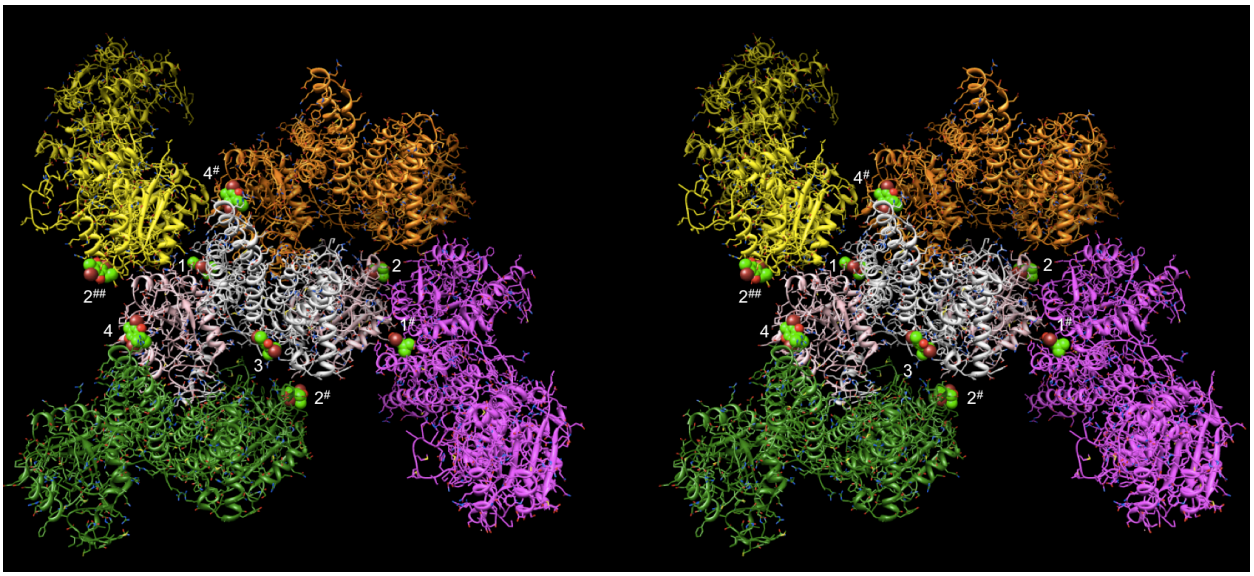

Figure S5. Cross-eye stereo view of lattice interactions in the crystal structure of the *S. elongatus* KaiA dimer:DBMIB complex. The color code of the original KaiA dimer (N-terminal domains are pink and C-terminal domains are gray), protein symmetry mates and DBMIB molecules is identical to that in **Figure 2** of the main manuscript. The four unique DBMIB molecules are numbered 1 to 4 and symmetry mates are marked by #. Each KaiA dimer exhibits contacts to 8 DBMIB molecules, whereby the interactions to N-terminal domains are more intimate than those to C-terminal ones. DBMIB 3 constitutes an exception in that it is only coordinated to the C-terminal domains of a single KaiA dimer. The drawing was generated with the program UCSF Chimera.[13]

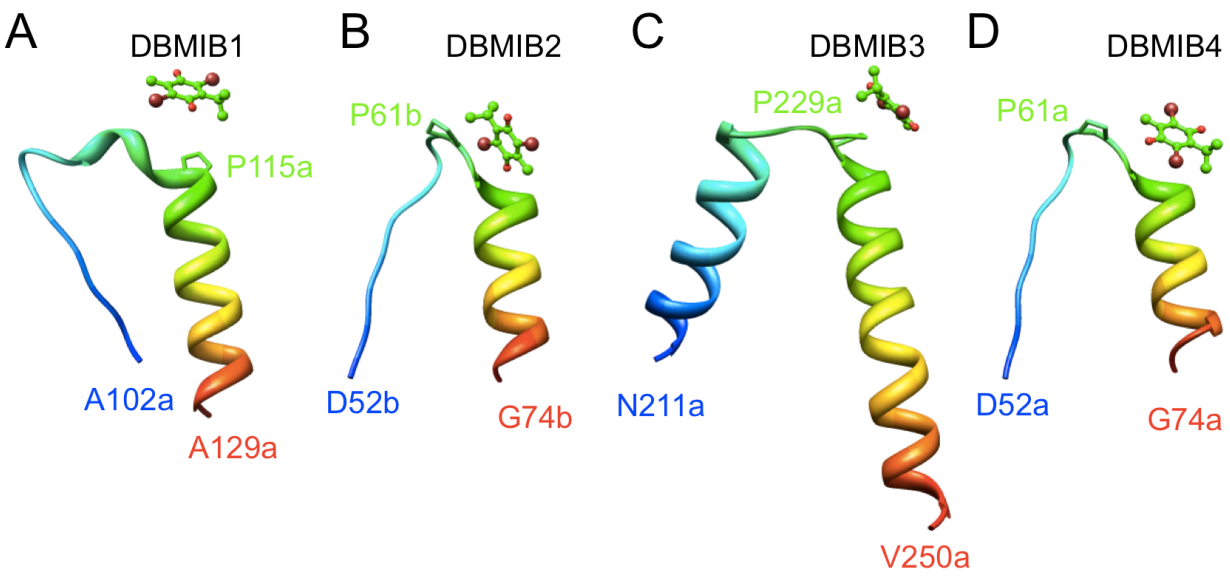

Figure S6. Common topology of DBMIB binding sites. In all four cases, the quinone analog sits adjacent to the N-terminus of an α-helix that is preceded by a turn involving proline. For (A) DBMIB1, (B) DBMIB2 and (D) DBMIB4 bound to N-KaiA, the turn is between a β-strand and the α-helix, whereas (C) DBMIB 3 bound to C-KaiA is lodged next to a turn between α-helices. Portions of the Cα-atom chain are shown in ribbon mode with the first and last residues as well as proline labeled. The drawing was generated with the program UCSF Chimera.[13]

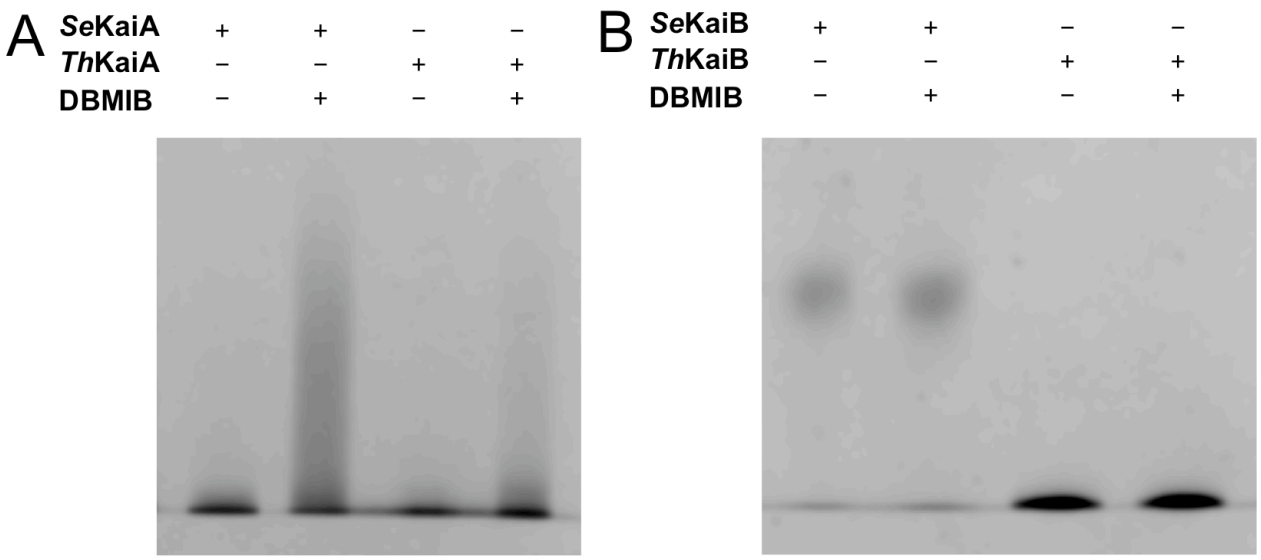

Figure S7. Native PAGE assay for aggregation of the (A) KaiA proteins and (B) KaiB proteins from *S. elongatus* (*Se*) and *T. elongatus* (*Th*) in the absence (left lane) and presence (right lane) of oxidized DBMIB. Only KaiA proteins exhibit aggregation upon addition of DBMIB whereas KaiB proteins remain unaffected.

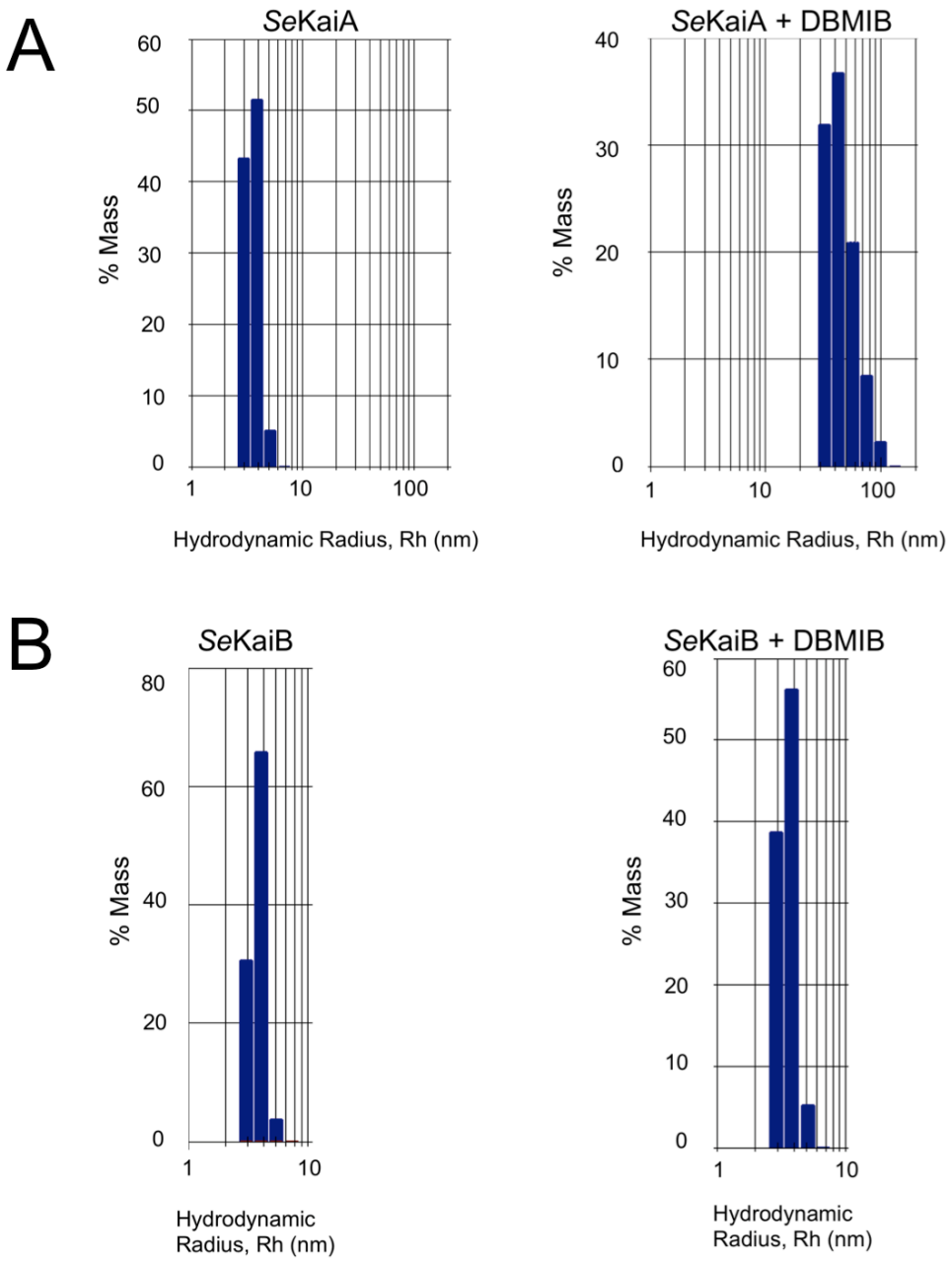

Figure S8. Dynamic light scattering assay for aggregation of the (A) KaiA protein and (B) KaiB protein from *S. elongatus* (*Se*) in the absence (left) and presence (right) of oxidized DBMIB. Only KaiA protein exhibits aggregation upon addition of DBMIB whereas KaiB protein remains unaffected.

References

1. Mori, T., Williams, D. R., Bryn, M., Qin, X., Egli, M., Mchaourab, H., Stewart, P. L., and Johnson, C. H. Elucidating the ticking of an in vitro circadian clockwork. *PLoS Biol*., **2007**, 5, e93.

2. Pattanayek, R., Williams, D. R., Rossi, G., Weigand, S., Mori, T., Johnson, C. H., Stewart, P. L., and Egli, M. Combined SAXS/EM based models of the *S. elongatus* posttranslational oscillator and its interactions with the output His-kinase SasA. *PLoS ONE*, **2011**, *6*, e23697.

3. Pattanayek, R., Williams, D. R., Pattanayek, S., Xu, Y., Mori, T., Johnson, C. H., Stewart, P. L., and M. Egli (2006) Analysis of KaiA-KaiC protein interactions in the cyanobacterial circadian clock using hybrid structural methods. *EMBO J.*, **2006**, *25*, 2017-2028.

4. Pattanayek, R., Williams, D. R., Pattanayek, S., Mori, T., Johnson, C. H., Stewart, P. L., and Egli, M. Structural model of the circadian clock KaiB-KaiC complex and mechanism for modulation of KaiC phosphorylation. *EMBO J.*, **2008**, *27*, 1767-1778.

5. Ye, S., Vakonakis, I., Ioerger, T.R., LiWang, A.C., and Sacchettini, J. C. Crystal structure of circadian clock protein KaiA from *Synechococcus elongatus*. *J. Biol. Chem*., **2004**, *279*, 20511-20518.

6. Otwinowski, Z., and Minor, W. Processing of X-ray diffraction data collected in oscillation mode. *Meth. Enzymol.*, **1997**, *276***,** 307-326.

7. Brunger, A. T., Adams, P. D., Clore, G. M., DeLano, W. L., Gros, P., Grosse-Kunstleve, R. W., Jiang, J. S., Kuszewski, J., Nilges, M., Pannu, N. S., Read, R. J., Rice, L. M., Simonson, T., and Warren, G. L. Crystallography & NMR system: A new software suite for macromolecular structure determination. *Acta Cryst. D*, **1998**, *54***,** 905-921.

8. Adams, P. D., Afonine, P. V., Bunkoczi, G., Chen, V. B., Davis, I. W., Echols, N., Headd, J. J., Hung, L.W., Kapral, G. J., Grosse-Kunstleve, R. W., McCoy, A. J., Moriarty, N. W., Oeffner, R., Read, R. J., Richardson, J. S., Terwilliger, T. C., and Zwart, P. H. PHENIX: a comprehensive Python-based system for macromolecular structure solution. *Acta Cryst. D*, **2010**, *66*, 213-221.

9. Emsley, P., and Cowtan, K. Coot: model-building tools for molecular graphics. *Acta Cryst. D*, **2004**, *60*, 2126-2132.

10. Wood, T. L., Bridwell-Rabb, J., Kim, Y.-I., Gao, T., Chang, Y.-G., LiWang, A., Barondeau, D. P., and Golden, S. S. The KaiA protein of the cyanobacterial circadian oscillator is modulated by a redox-active cofactor. *Proc. Natl. Acad. Sci. U.S.A.*, **2010**, *107*, 5804-5809.
11. Rasband, W. S., ImageJ, U. S. National Institutes of Health, Bethesda, Maryland, USA, http://imagej.nih.gov/ij/, 1997-2012.
12. DeLano, W. L. The PyMol Molecular Graphics System. DeLano Scientific LLC, San Carlos, CA, USA. http://www.pymol.org.
13. Pettersen, E. F., Goddard, T. D., Huang, C. C., Couch, G. S., Greenblatt, D. M., Meng, E. C., and Ferrin, T. E. UCSF Chimera, a visualization system for exploratory research and analysis. *J. Comp. Chem.*, **2004**, *25*, 1605-1612.